NACA RM A55A06a

RESEARCH MEMORANDUM

A COMPARISON OF TWO METHODS FOR COMPUTING THE WAVE DRAG OF WING-BODY COMBINATIONS

By Alberta Alksne

Ames Aeronautical Laboratory
Moffett Field, Calif.

NATIONAL ADVISORY COMMITTEE
FOR AERONAUTICS
WASHINGTON
April 7, 1955

NACA RM A55A06a

NATIONAL ADVISORY COMMITTEE FOR AERONAUTICS

RESEARCH MEMORANDUM

A COMPARISON OF TWO METHODS FOR COMPUTING THE WAVE DRAG OF WING-BODY COMBINATIONS

By Alberta Alksne

SUMMARY

Computations of wave drag based on linearized theory have been performed for four wing-body combinations tested by Whitcomb and reported in NACA RM L52H08. The results are shown in comparison with the experimental data. Two computational techniques for evaluating the integrals in the theoretical expressions for wave drag are discussed, namely, Fourier series and graphical or numerical integration. Advantages and disadvantages of each are pointed out.

INTRODUCTION

Recently Whitcomb (ref. 1) has postulated, and demonstrated experimentally, that the wave drag of a system of wings and bodies at a free-stream Mach number very near unity is approximately the same as that of an equivalent body of revolution, that is, of a body of revolution having the same streamwise distribution of cross-sectional area. A similar conclusion was reached by Hayes (ref. 2) as a limiting case of linear theory as the Mach number goes to 1, and can be expressed by the formula given by Heaslet, Lomax, and Spreiter (ref. 3).

$$D_{(M_0 \to 1^+)} = -\frac{\rho_0}{4\pi} \int_0^l \int_0^l f'(x_1) f'(x_2) \ln|x_1 - x_2| \, dx_1 dx_2 \qquad (1)$$

where $f'(x)$ is the derivative with respect to x of a source strength which is related to the system of wings and bodies under consideration, l is the over-all length of the system and $f(0) = f(l) = 0$.

For a slender body of revolution the source strength is proportional to the normal component of the stream velocity at the body surface, and sources of the appropriate strength may be placed on the x axis. Equation (1) then reduces to the following, which is also recognizable as von Kármán's formula for supersonic wave drag (ref. 4).

$$D_{(m\longrightarrow 1^+)}=\frac{\rho_o V_o^2}{4\pi}\int_o^l\int_o^l S''(x_1)S''(x_2)\ln|x_1 - x_2|dx_1dx_2 \qquad (2)$$

where $S''(x)$ is the second derivative with respect to x of the cross-sectional area intercepted by a plane perpendicular to the stream direction. For Mach numbers near 1 this formula can be used also for wing-body combinations, provided the area distribution is sufficiently smooth and appropriate conditions apply at the nose and tail.

In the case of supersonic flow, wing theory provides the following formula which is exact, within the limits of linear theory, for a plane nonlifting wing (ref. 2):

$$D = \frac{\rho_o}{8\pi^2}\int_o^{2\pi} d\theta \int_o^l\int_o^l f'(x_1,\beta\cos\theta)f'(x_2,\beta\cos\theta)\ln|x_1 - x_2|dx_1dx_2 \qquad (3)$$

where $\beta = \sqrt{M_o^2 - 1}$ and θ is the azimuth angle (see sketch (a)). In reference 2 relations are given between the velocity components on the wing and the source strengths, integrated along the lines on which $x + y\beta\cos\theta$ = constant and concentrated on the axis at the point of intersection.

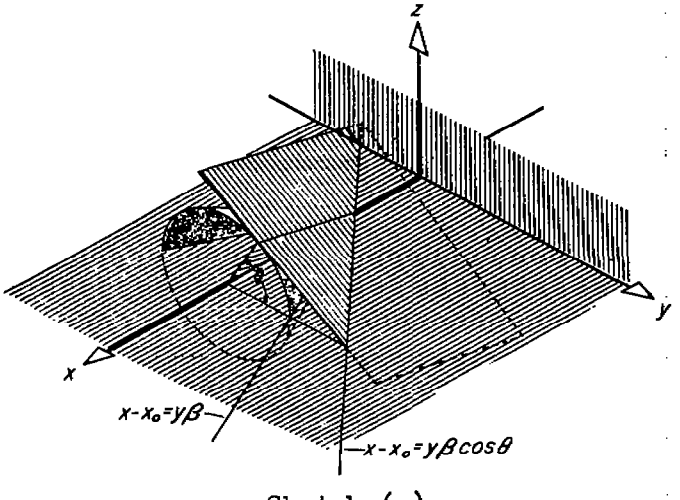

Sketch (a)

The problems of interest at present concern more complicated configurations made up of wings and bodies in combination, and in this case a difficulty arises in fixing the relations between the geometry of the configurations and the strengths of the singularities to be used in simulating the actual shape. In reference 5 R. T. Jones presented a supersonic area rule which is applicable to a large class of wing-body combinations including configurations involving thin

wings mounted centrally on slender bodies of revolution. In effect, the supersonic area rule introduces into equation (3) the approximate relation

$$f'(x,\beta \cos \theta) = S''(x_o,\beta \cos \theta)$$

where the primes indicate differentiation with respect to x, and where $S(x_o,\beta \cos \theta)$ is the projection normal to the stream direction of the cross-sectional area intercepted by a plane tangent at θ to the Mach cone whose vertex is at the point x_o on the x axis. Returning to sketch (a) one can see that the plane tangent to the Mach cone intersects the xy plane in the line $x - x_o = y\beta \cos \theta$. It was along such lines that the sources were integrated in the case of a plane, nonlifting wing discussed in reference 2.

The use of the above relation for $f'(x,\beta \cos \theta)$ makes it possible to rewrite equation (3) as follows:

$$D = -\frac{\rho_o V_o^2}{8\pi^2} \int_o^{2\pi} d\theta \int_o^l \int_o^l S''(x_1,\beta \cos \theta)S''(x_2,\beta \cos \theta)\ln|x_1 - x_2|\, dx_1 dx_2 \tag{4a}$$

After two integrations by parts, taking proper account of the singularities, and the use of the requirement that $S'(0) = S'(l) = 0$, this reduces to

$$D = \frac{\rho_o V_o^2}{8\pi^2} \int_o^{2\pi} d\theta \, \neq\!\!\int_o^l \neq\!\!\int_o^l \frac{S'(x_1,\beta \cos \theta)S'(x_2,\beta \cos \theta)dx_1 dx_2}{(x_1 - x_2)^2}$$

$$\equiv \frac{\rho_o V_o^2}{8\pi^2} \int_o^{2\pi} [I(\beta \cos \theta)]d\theta \tag{4b}$$

where $I(\beta \cos \theta)$ is defined by the double integral. Note the use of the symbol $\neq\!\!\int$ to indicate the "generalized principal part" as discussed by Heaslet and Lomax in reference 6.

The present paper applies the theoretical formulas given above to compute wave drag and discusses the technique of carrying out the analysis. Procedures for computing the area distributions, $S(x_o,\beta \cos \theta)$, and their derivatives, $S'(x_o,\beta \cos \theta)$, for a given configuration are discussed and certain convenient simplifications are studied. Two computational methods of evaluating the integrals are considered, namely, Fourier

[redacted]

analysis and numerical integration. The Fourier series method has been previously considered in references 5 and 7.

SYMBOLS

A	aspect ratio
$A_n(\beta \cos \theta)$	Fourier coefficients corresponding to S'; $\frac{2}{\pi} \int_0^{\pi} S'(x_o, \beta \cos \theta) \sin n\varphi \, d\varphi$
A_n	same as $A_n(\beta \cos \theta)$ (The parenthesis is omitted for convenience when it is not important to stress the functional nature of the symbol.)
a_n	Fourier coefficients corresponding to s'; $\frac{2}{\pi} \int_0^{\pi} s' \sin n\varphi \, d\varphi$
C_D	wave-drag coefficient, $\frac{D}{\frac{\rho_o V_o^2}{2} S_W}$
c or $c(y)$	local chord of wing
D	wave drag
$f(x)$	source strength at x
I or $I(\beta \cos \theta)$	value of double integral in equation (4b) (see also eq. (10))
K	maximum height of peak of an arbitrary curve
l	over-all length of wing-body system
M_o	free-stream Mach number
m,n	integers
r	radius of body
r_o	maximum radius of body
S	same as $S(x_o, \beta \cos \theta)$ or $S(x)$ (The parenthesis is omitted for convenience when it is not important to stress the functional nature of the symbol.)

[redacted]

$S(x)$	cross-sectional area in plane perpendicular to free-stream direction
$S(x_o, \beta \cos \theta)$	projection on plane $x = x_o$ of cross-sectional area in a plane tangent at θ to a Mach cone originating at x_o (see sketch (a))
S_W	area of wing plan form including that part masked by the body
s	component of S; $S = s_1 + s_2 + \cdots$
t	local thickness of wing (twice the ordinate of the upper surface)
$\frac{t}{c}$	local thickness ratio of wing
V_o	free-stream velocity
x,y,z	Cartesian coordinates (see sketch (a))
x_o	vertex of Mach cone (see sketch (a))
y_1 or y_2	limits of integration
β	$\sqrt{M_o^2 - 1}$
δ	half width of peak of an arbitrary curve
θ	azimuth angle, angle in an x = constant plane which identifies a point on the Mach cone (see sketch (a))
ρ_o	free-stream density
φ	$\arccos\left(1 - \frac{2x_o}{l}\right)$
φ_o	value of φ at maximum point of peak of an arbitrary curve
$'$	differentiation with respect to x or x_o

DISCUSSION OF COMPUTATIONAL METHODS

Generally speaking, the formulas for wave drag given in the Introduction, specifically, equations (2), (4a), and (4b), cannot be expected to give a realistic magnitude of the wave drag at a Mach number of 1,

since the pressures, in linear theory, become infinite. However, as the Mach number increases the agreement should improve. The more slender the configuration the narrower should be the range of Mach numbers showing poor agreement between theoretical and measured wave drag.

Furthermore, difficulties can be expected to arise in the use of equations (2) and (4) whenever there are discontinuities in S' or S''. Some singularities are, of course, integrable. For instance, so simple a configuration as a Sears-Haack body possesses a singularity in S'' at the nose, yet integration produces a finite drag. Any configuration with a step in the S' curve has an infinite value of $I(\beta \cos \theta)$ in equation (4b) for every value of θ for which the step occurs. Such a step, for instance, occurs when the leading edge of a wing lies along a Mach line unless the leading edge is cusped. It is possible to obtain finite drag, using equation (4b), for configurations having a finite number of logarithmic singularities in $I(\beta \cos \theta)$, but not for a configuration for which the infinity extends over a finite range of θ.

The first and most difficult step in evaluating the wave drag is the performance of the double integration with respect to x, that is, the evaluation of $I(\beta \cos \theta)$. Difficulties arise from several sources. First, the evaluation of $S'(x_o, \beta \cos \theta)$ is not simple for a configuration of practical interest. Second, this function, when found, is not generally known in analytic form and some means of approximating it by an analytical expression is desirable as a means of avoiding detailed numerical calculations. Third, the integrand has a singularity at $x_1 = x_2$ and therefore is not suitable for direct numerical integration in this form.

Ways of surmounting these difficulties are discussed in the following sections.

Computation of $S'(x_o, \beta \cos \theta)$

Before undertaking the computation of $S'(x_o, \beta \cos \theta)$ as defined following equation (3), it is desirable to make a further simplifying assumption. If the system consists of a body combined with a thin wing lying in the xy plane, as was the case for the configurations studied herein, it is assumed satisfactory to replace the plane tangent to the Mach cone by a plane perpendicular to the xy plane through the line $x - x_o = y\beta \cos \theta$. It is then possible, as was done for reference 7, to plot the ordinates of the wing and body at points in this plane, project on the plane $x = x_o$, integrate to get $S(x_o, \beta \cos \theta)$, and plot the results as a function of x_o. The resulting data can then be differentiated graphically or numerically to obtain $S'(x_o, \beta \cos \theta)$. However, such a differentiation is difficult to perform accurately and care must

be taken in fairing the resulting points if a realistic picture of $S'(x_o, \beta \cos \theta)$ for the configuration is to be obtained.

In the following paragraphs a procedure is shown for computing $S'(x_o, \beta \cos \theta)$ without resorting to numerical differentiation except in certain particular cases. It consists in setting up an analytical expression for $S(x_o, \beta \cos \theta)$ which can be differentiated analytically, thus making both S and S' readily available.

The wing-body system to be studied is first broken down into its various components. For instance in the present cases the body and each wing panel are considered separately. The curve $S(x_o, \beta \cos \theta)$ or $S'(x_o, \beta \cos \theta)$ of the whole system is then the point-by-point sum of the curves for the components.

Calculation of $S'(x_o, \beta \cos \theta)$ for a body of revolution.- To obtain $S'(x_o, \beta \cos \theta)$ analytically for even a simple body of revolution is somewhat difficult and it becomes much more so for an irregular indented body. However, it has been assumed in the present case that for a slender body a further approximation is permissible at Mach numbers near 1, namely, $S'(x_o)$ can be substituted for $S'(x_o, \beta \cos \theta)$, which means that only cuts perpendicular to the stream direction need be used. This is in accordance with slender-body theory.

As will be shown later in this paper, unless the body modifications are slight and gradual the wave-drag results will be somewhat different, depending on whether normal cuts or slant cuts are used in the computation of S' of the body. A difference will appear when the abruptness of the body modification results in a significant difference between the area in a plane normal to the stream direction and the projection on that plane of the area in a plane at an oblique angle having the same intersection with the x axis. This is contrary to the assumptions of slender-body theory and the question of whether or not the added complexity of using slant cuts through a body of revolution is justifiable for $M_o > 1$ has not been determined.

When the radius of a body of revolution is known as a function of x_o, both $S(x_o)$ and $S'(x_o)$ are readily obtained. For a body which has been modified in accordance with Whitcomb's area rule to give the same $S'(x_o)$ at $M_o = 1$ for the wing-body combination as for the unmodified or basic body alone, the relation of the radius to x_o in the modified region usually cannot be expressed as a simple function, but in that case $S'(x_o)$ of the modified region is simply $S'(x_o)$ of the basic body less $S'(x_o)$ of the wings. Thus for this type of modification, no numerical differentiation is required to obtain $S'(x_o)$ of the modified region if $S'(x_o)$ of the wings can be computed directly, and if $S'(x_o)$ of the basic body is known.

[redacted]

Calculation of $S'(x_o,\beta \cos \theta)$ for a wing panel.- To obtain $S(x_o,\beta \cos \theta)$ and $S'(x_o,\beta \cos \theta)$ for a wing panel for which the thickness ratio t/c and plan form can be expressed as functions of x and y, it is only necessary to make the substitution

$$x = x_o + y\beta \cos \theta$$

$$y = y$$

so that $\frac{t}{c}(x,y)$ can be replaced by $\frac{t}{c}(x_o,y,\beta \cos \theta)$. Then

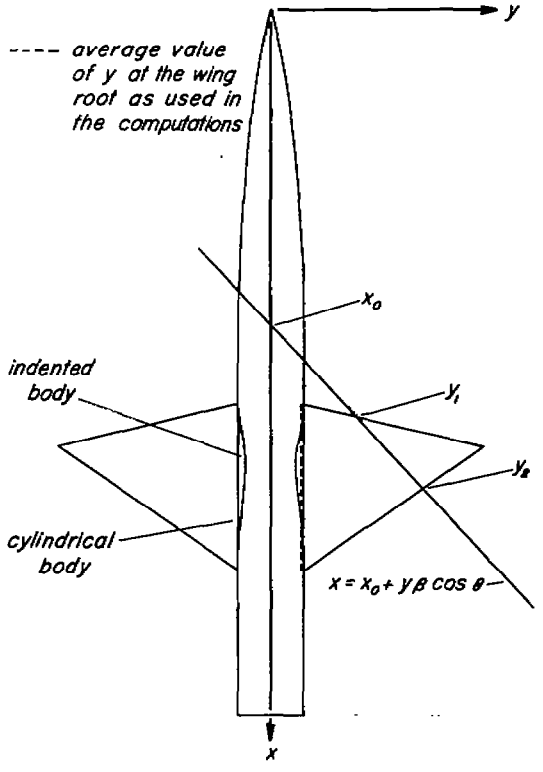

Sketch (b)

$$S(x_o,\beta \cos \theta) = \int_{y_1}^{y_2} \left[\frac{t}{c}(x_o,y,\beta \cos \theta) \right] [c(y)]dy$$

and

$$S'(x_o,\beta \cos \theta) = \frac{\partial}{\partial x_o} S(x_o,\beta \cos \theta)$$

$$= \frac{\partial}{\partial x_o} \int_{y_1}^{y_2} \left[\frac{t}{c}(x_o,y,\beta \cos \theta) \right] [c(y)]dy$$

where c is the local chord and the limits y_1 and y_2 are functions of x_o and $\beta \cos \theta$ determined from the plan form (see sketch (b)).

The differentiation can be performed as follows:

$$S'(x_o,\beta \cos \theta) = \left[\frac{\partial}{\partial x_o} y_2(x_o,\beta \cos \theta) \right] \left[\frac{t}{c}(x_o,y_2,\beta \cos \theta) \right] [c(y_2)] -$$

$$\left[\frac{\partial}{\partial x_o} y_1(x_o,\beta \cos \theta) \right] \left[\frac{t}{c}(x_o,y_1,\beta \cos \theta) \right] [c(y_1)] +$$

$$\int_{y_1}^{y_2} \frac{\partial}{\partial x_o} \left[\frac{t}{c}(x_o,y,\beta \cos \theta) \right] [c(y)]dy \qquad (5)$$

[redacted]

The only instances in which the first two terms on the right will not vanish occur when one of the limits is a function of x_o where the thickness ratio has at the same time a nonzero value. This will occur at the wing root when the wing is attached to a body of varying radius as in an indented region. If the variation of r with x_o is small, it is permissible to use a constant, average value of r, or y, at the juncture of the wing and body, thus completing the elimination of the first two terms. This simplification, which amounts to the assumption of a straight wing root, was used in the present computations and investigation showed that the error introduced was negligible for the cases considered.

It is usually possible to devise an approximate expression for the thickness ratio of the wing, in terms of x and y, for which the integral in equation (5) can be evaluated analytically. If a single simple expression cannot be found, no great complication is introduced by using different expressions for different regions of the wings. This technique permits direct computation of $S'(x_o, \beta \cos \theta)$ for each wing panel without resort to graphical differentiation. In fact, the computation of S' may be no more difficult than the computation of S.

Evaluation of Wave-Drag Integrals by Fourier Series

The function $S'(x_o, \beta \cos \theta)$ for a wing-body combination can generally be determined at as many points as may be required, but cannot, except in special cases, be expressed in a simple analytical form. However, it can be approximated by a Fourier series:

$$S'(x_o, \beta \cos \theta) = \sum_{n=1}^{\infty} A_n(\beta \cos \theta) \sin n\varphi$$

where

$$\varphi = \arccos\left(1 - \frac{2x_o}{l}\right)$$

and

$$A_n(\beta \cos \theta) = \frac{2}{\pi} \int_0^{\pi} S'(x_o, \beta \cos \theta) \sin n\varphi \, d\varphi$$

where the notation $A_n(\beta \cos \theta)$ indicates that the coefficients are functions of both Mach number and azimuth angle.

[redacted]

When the Fourier series has been substituted for $S'(x_o, \beta \cos \theta)$ in equation (4b), the first two integrations can be performed to give

$$D = \frac{\rho_o V_o^2}{16} \int_o^{2\pi} \sum_{n=1}^{\infty} n \left[A_n(\beta \cos \theta)\right]^2 d\theta \tag{6}$$

At $M_o = 1$, since $\beta \cos \theta = 0$ for all values of θ, equation (4a) reduces to equation (2) and

$$D_{(M_o \longrightarrow 1^+)} = \frac{\pi \rho_o V_o^2}{8} \sum_{n=1}^{\infty} n (A_n)^2 \tag{7}$$

(See refs. 7 and 8.)[1] For other Mach numbers it is usually convenient to perform the final integration graphically.

The Fourier series method of performing the first two integrations is admirably suited to the use of punched-card computing machines or other mechanized computing systems as long as the $S'(x_o, \beta \cos \theta)$ curves are smooth and without sharp peaks. When such machines are available and the information is provided in the form of plots of $S'(x_o, \beta \cos \theta)$ vs. φ, the evaluation of the double integral for each case requires only about 2 hours.

One drawback of the above method is that if the S' curve has sharp peaks, the Fourier series will not be able to represent the function adequately in a reasonable number of terms. For the present analysis 24 terms were available and in some cases that was not enough to bring the series to convergence. In such a case the solution, per se, is clearly not valid. Various checks are available to determine the convergence of the series for a particular case though little can be said in general. The coefficients can be used to recompute an S' curve to compare with that originally provided, or the $\sum_{n=1}^{m} n(A_n)^2$ can be plotted against m and the trend noted, or some forecast of the number of terms required for convergence can be obtained by a method such as that shown in the next section.

[1]Note that in reference 8 the Fourier coefficients differ by π from those defined herein.

[redacted]

Further Investigation of the Fourier Series Method

The Fourier series method has been used in reference 7 as well as by the present author for the computation of wave drag from equation (4b), and it is subject to the danger already pointed out of failure of the series to converge in the available number of terms. For this reason a further study was undertaken, leading to a clearer picture of the relation between $S'(x_0, \beta \cos \theta)$ and the corresponding Fourier coefficients. In addition, the technique developed for this study was used in evaluating the simplifications mentioned in the section on computation of $S(x_0, \beta \cos \theta)$ and $S'(x_0, \beta \cos \theta)$.

Computation of Fourier coefficients for isolated peaks.- If the curve to be represented is considered as the sum of a number of components

$$S' = s_1' + s_2' + s_3' + \cdots$$

the corresponding Fourier series is then the sum of the series representing the components, from which it follows that

$$A_n = a_{n_1} + a_{n_2} + a_{n_3} + \cdots$$

where

$$a_{n_1} = \frac{2}{\pi} \int_0^{\pi} s_1' \sin n\varphi \, d\varphi$$

Now if a component s_1' consists of a single peak (see sketch (c)), the analytical form of the general term for the coefficients of a Fourier sine series representing s' can be stated as follows: If a peak of height K and width 2δ is located at $\varphi = \varphi_0$ then, assuming the peak to be an isosceles triangle, application of the Fourier formula yields

$$a_n = \frac{4K}{\pi \delta n^2} (1 - \cos n\delta) \sin n\varphi_0 \quad (8)$$

or, assuming the peak to be the upper half of a sine wave

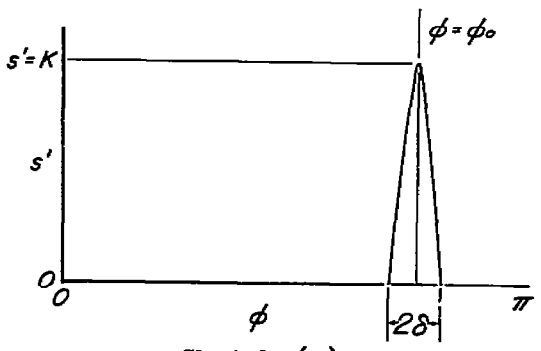

Sketch (c)

[redacted]

$$a_n = \frac{2K}{\delta n^2}\left[\frac{1}{(\pi/2n\delta)^2 - 1}\right]\cos n\delta \sin n\varphi_o \qquad (9)$$

and

$$\lim_{n\to(\pi/2\delta)} a_n = \frac{K \sin n\varphi_o}{n}$$

It is useful to note that both expressions divide naturally into three parts: a periodic function whose period depends on φ_o, a periodic function whose period depends on δ, and a damping factor of the order of $1/n^2$. For a sharp narrow peak ($\delta << \pi$), cos $n\delta$ is a very long period function and, when combined with the damping factor, it provides an envelope within which the shorter period oscillations due to sin $n\varphi_o$ are confined. This permits an estimate of the maximum possible size of a component a_n for any value of n. Sketches (d-1) and (d-2) show the coefficients a_{n_1} and the envelope for a peak of height K = -0.85

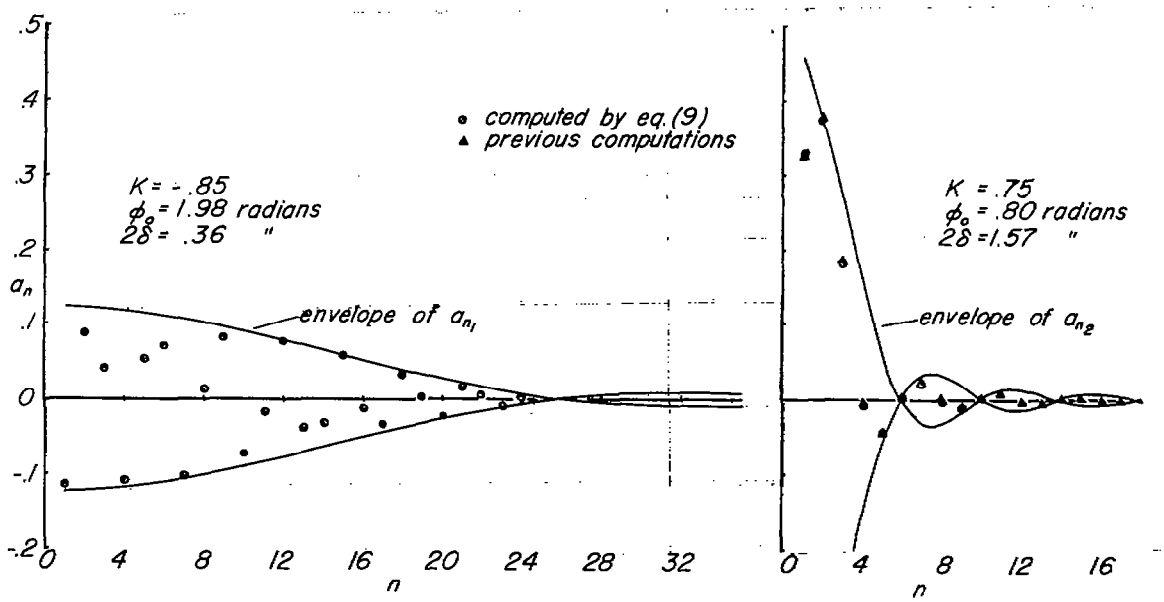

Sketch (d-1) Sketch (d-2)

[redacted]

and width $2\delta = 0.36$ radians located at $\varphi_0 = 1.98$ radians, compared with a similar plot of the coefficients a_{n_2} and envelope, for a peak of height $K = 0.75$ and width $2\delta = 1.57$ radians located at $\varphi_0 = 0.8$ radians. Note that for $n > 5$ the sharp peak ($2\delta = 0.36$) would play the dominant role in the sum $A_n = a_{n_1} + a_{n_2}$. (The coefficients a_{n_2} had previously been computed on the punched-card computing machines and are plotted in sketch (d-2) as a check on the accuracy of this technique.)

It is encouraging from the point of view of the general usefulness of the Fourier method of computing wave drag that, for such peaks as assumed above, if K is finite and $\delta \neq 0$, then $\sum_1^\infty n(A_n)^2$ will always converge in a fashion related to $1/n^3$ making it possible to judge roughly the number of terms required.

Application of the method of isolated peaks to the study of convergence.- It was found feasible, when a curve of S' was largely smooth with one or two sharp peaks, to determine with the help of equation (9) at what point the coefficients due to the smooth part would become negligible, and, from that point on, to compute coefficients due to each of the sharp peaks separately by either equation (8) or equation (9). This was done out to $n = 35$ for several cases, and to $n = 40$ for one case, where the series $\sum n[A_n(\beta \cos \theta)]^2$ failed to converge within the 24 terms available from the punched-card computing machines. Sketch (e) shows a typical plot of $\sum_{n=1}^{m} n(A_n)^2$ against m. Additional points beyond $m = 24$ are plotted with flags on the symbols.

It must be remembered that, after computing coefficients separately for more than one component of a curve, it is necessary to add the coefficients together to get a total coefficient for each value of n before performing the squaring and summing operations. Otherwise the interference between the components will be lost.

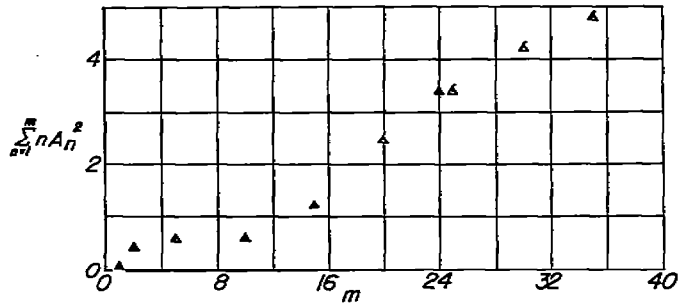

Sketch (e)

The phenomenon shown in sketch (e) of apparent convergence at one point in the series followed by further increase in $\sum_{n=1}^{m} n(A_n)^2$ with

[redacted]

additional terms can be seen from consideration of the above technique to be due, at least in some cases, to the interaction of two or more peaks, resulting in "beats" in the total coefficients A_n where the component coefficients $a_{n_1}, a_{n_2}, \ldots$ cancel each other over a certain range and later reinforce each other.

In order to assure a valid solution the series should be carried far enough to fit the S' curve in all its essential parts but not far enough to pick up extraneous effects from small variations in the curve such as those due to numerical or graphical differentiation.

Application of the method of isolated peaks to the computation of Fourier coefficients for components added to a basic configuration.- In situations where it is desired to add a component to a system of wings and bodies for which the drag has already been computed by Fourier series, that is, for which the Fourier coefficients are already available, it is possible, using the technique described above, to estimate the effect of the addition. The gradient of cross-sectional area for the addition is plotted against the φ for the entire configuration, the Fourier coefficients are computed separately and added to the original set. This method was used in evaluating the effect of using slant cuts through the body for Mach numbers greater than 1.

In the section on computation of $S'(x_o, \beta \cos\theta)$ for a wing-body combination, two simplifications were proposed. One, the use of a constant average value of y (straight wing root) as one of the limits of integration in place of the more accurate variable limit was found to have a negligible effect on the $S'(x_o, \beta \cos\theta)$ curve for the cases considered. The other, the substitution of $S'(x_o)_{\beta \cos\theta = 0}$ instead of $S'(x_o, \beta \cos\theta)$ for the body of revolution in computing $S'(x_o, \beta \cos\theta)$ of the system (i.e., the use of normal cuts through the body regardless of Mach number) was found to have a pronounced effect on the curve of $S'(x_o, \beta \cos\theta)$ of the whole configuration when the changes in cross-sectional area of the body were not gradual.

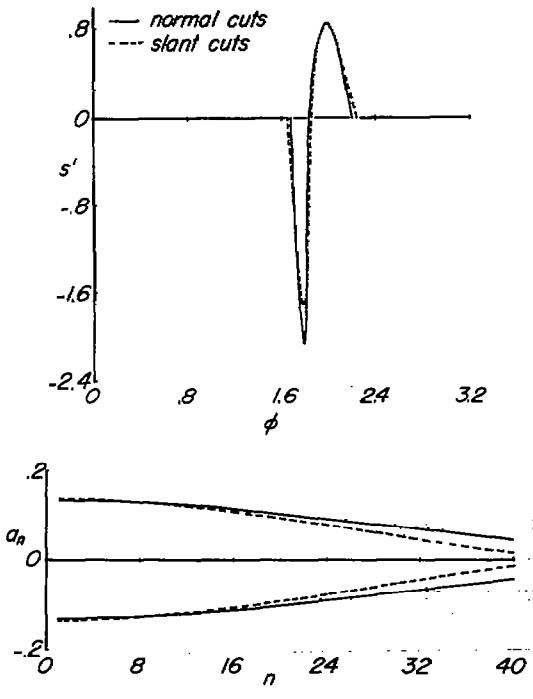

Sketch (f)

Sketch (f) shows the extent to which the use of slant cuts altered the components of the S' curve associated with the indented region of the body and the resulting change in the envelope

[redacted]

of the Fourier coefficients corresponding to the negative peak. This change resulted in more rapid convergence and consequently smaller coefficients for large values of n when slant cuts were used.

The indication is that this simplification, the substitution of $S'(x_0)$ of the body for $S'(x_0, \beta \cos \theta)$ of the body for $M_0 > 1$, should receive careful consideration before it is used even though it is sanctioned by slender theory. If slant cuts through a body of revolution give results that differ significantly from those obtained using straight cuts, then computation of the wave drag for the body probably exceeds the bounds of the theory.

Evaluation of Wave-Drag Integrals by Numerical Integration

The double integral in the form given in equation (4) is unsuited to numerical or graphical integration because of the presence of a singularity at $x_1 = x_2$. An alternate form is displayed by M. Robert Legendre (ref. (9)) as follows:

$$I = \frac{1}{2} \int_0^l \int_0^l \frac{[S'(x_1, \beta \cos \theta) - S'(x_2, \beta \cos \theta)]^2}{(x_1 - x_2)^2} dx_1 dx_2 +$$

$$l \int_0^l \frac{[S'(x, \beta \cos \theta)]^2}{x(l - x)} dx \qquad (10)$$

Note that in this form no singularity appears at $x_1 = x_2$ unless $S''(x) = \infty$.

Within the limitations of the theory, the drag of any system of wings and bodies for which $S'(x_0, \beta \cos \theta)$ is available (either as a curve or a table of numerical values) can be computed directly using equations (10) and (4b), or a further adjustment can be made to permit the separate calculation of interference drag and the drag of the components.

As suggested in connection with the study of the Fourier analysis, the curve S' may be considered as the sum of various components $s_1' + s_2' + s_3' + \ldots$ and it can be substituted into equation (10) in

that form. Since the systems for which the wave drag is being computed frequently consist of a wing and a body, or a basic configuration and a modification, it is convenient to divide the derivative of the area distribution into two parts, thus: If $S'(x) = s_1'(x) + s_2'(x)$, equation (10) can be written

$$I = \frac{1}{2}\int_0^l \int_0^l \frac{[s_1'(x_1) - s_1'(x_2)]^2}{(x_1 - x_2)^2}\,dx_1dx_2 + l\int_0^l \frac{[s_1'(x)]^2}{x(l-x)}\,dx +$$

$$\frac{1}{2}\int_0^l \int_0^l \frac{[s_2'(x_1) - s_2'(x_2)]^2}{(x_1 - x_2)^2}\,dx_1dx_2 + l\int_0^l \frac{[s_2'(x)]^2}{x(l-x)}\,dx +$$

$$\int_0^l \int_0^l \frac{[s_1'(x_1) - s_1'(x_2)][s_2'(x_1) - s_2'(x_2)]}{(x_1 - x_2)^2}\,dx_1dx_2 +$$

$$2l\int_0^l \frac{s_1'(x)s_2'(x)}{x(l-x)}\,dx \qquad (11)$$

where the first two terms lead to the wave drag of the component associated with $s_1'(x)$, the next two terms to that associated with $s_2'(x)$, and the last two terms, which need not be positive, represent the interference between the two. If the wave drag of the separate components is known, either from previous computations or from test data, only the cross-product terms remain to be computed to give the total wave drag.

PRESENTATION OF RESULTS AND COMPARISON WITH EXPERIMENT

Computations of wave drag have been performed for four of the wing-body combinations tested by Whitcomb and the results are presented herein in comparison with the experimental wave drag. The Appendix together with figure 1 give the pertinent data to describe each configuration.

Figures 2 and 3 show typical examples of the S' curves for the various configurations. In all cases S' was computed by analytical methods. Any irregularities, therefore, are due to the combination of the component parts of the configuration and not to the inaccuracies of numerical differentiation. It is interesting to notice the difference in the height and sharpness of the peaks in S' for the two different wings.

[redacted]

All the configurations shown in figure 1 are sufficiently slender to fall within the range of applicability of the theory, and it would be expected that for all of them the wave-drag computations should have equal chance of success. The basic bodies are the same (cylindrical behind $x = l/2$), the aspect ratios are the same, and the wings are both reasonably thin with respect to their own chord length and with respect to the body radius. However, closer attention reveals that the body modification that goes with wing B (i.e., the indentation which is required to cancel the wing area exactly at $M_0 = 1$) is not a gradual one, but is concentrated in a very small longitudinal distance. This is particularly noticeable in comparison with the indentation for wing A and is even more obvious when the S' curves of the two configurations are compared.

The partial sums $\sum_{n=1}^{m} n[A_n(\beta \cos \theta)]^2$ have been plotted against m up to $m = 24$ in each case and are shown in figures 4 and 5 for the same values of $\beta \cos \theta$ as in figures 2 and 3. It should be noted that there is a marked failure of the series to converge within 24 terms in several cases for wing B and that these coincide with the cases of high, sharp peaks in $S'(x_0, \beta \cos \theta)$. For certain cases where convergence was poor, additional terms of the series were computed using equation (8) or (9), and the summation including these terms is plotted in figures 4 and 5 with flags on the symbols.

In all cases considered the wave drag has been computed from the partial sums to $n = 24$, regardless of convergence, by plotting $\sum_{n=1}^{24} n[A_n(\beta \cos \theta)]^2$ against θ and integrating graphically from 0 to 2π. The plots of $\sum_{n=1}^{24} n[A_n(\beta \cos \theta)]^2$ against θ are shown in figures 6 and 7(a). For several cases where the series failed to converge for wing B, the additional terms were used and the revised summation is plotted against θ in figure 7(b). The wave-drag coefficient, C_D, is plotted against Mach number in figures 8 and 9. Note that in figure 9 there are curves corresponding to both summations. In figure 8 there is only one set of curves since the convergence within 24 terms was satisfactory. Figure 8 shows as good agreement as can be expected between theory and experiment for wing A, both on the basic and on the modified body. As in reference 7, the agreement is poor at $M_0 = 1$ but improves with increasing Mach number. For wing B (fig. 9) the agreement is poor for Mach numbers near 1 for the wing on the basic body but the theoretical curves approach the experimental with increasing Mach number, reaching good agreement for Mach number greater than 1.06. For wing B on the indented body there is fairly good agreement near a Mach number of 1.

[redacted]

Good agreement at a Mach number of 1 for a straight-wing model optimized for $M_o = 1$ was also found in reference 10. The agreement between theory and experiment for wing B on the indented body becomes less satisfactory as the Mach number increases. However, there is some question concerning the experimental data for higher Mach numbers. For the range of Mach numbers presented it is believed possible that reflected waves from the tunnel walls could have influenced the measured drag coefficients for the modified bodies. In reference 11 such an effect was found to exist.

It is interesting that the range of greatest disagreement between theory and experiment corresponds with the range of poor convergence, that is, with the range in which the S' curves are characterized by excessively high peaks. Since it is to be expected that the use of slant cuts through the modified region will reduce the height of the peaks, the wave drag for wing B on the indented body has been recomputed using slant cuts through the body for the highest Mach number considered, namely, 1.1. Figure 10 shows the summation plotted against m and against θ. The resulting values of the wave-drag coefficient have been plotted in figure 9. The circle marks the result using 24 terms and the flagged circle, the result using 35 terms. Note that the more rapid convergence due to the use of slant cuts has made a considerable difference, about 18 percent in the latter case, although the difference within 24 terms is slight. The appearance of a difference due to using slant cuts indicates the possibility that the bounds of the theory have been exceeded.

As a test of the practicability of using a numerical integration technique, sample computations have been performed using both equations (10) and (11). The results are plotted in figures 8 and 9 for comparison with those from the Fourier analysis. Attention is called to the fact shown in figure 9 that the wave drag computed by this method for wing B on the basic body is significantly higher than that computed by the partial sums of the Fourier series using 24 terms, and that the use of additional terms of the Fourier series improves the agreement between the two methods although increasing the disagreement with experiment. However, it should be remembered that if the series used to compute the wave drag has not converged reasonably well within the number of terms used, any agreement with experiment may be fortuitous (possibly due to the influence of factors such as boundary layer not considered in the theory). Note that in figure 8 two values are plotted for $M_o = 1$ for the wing on the indented body. The point indicated by a triangle was computed by equation (10). For the point marked by a square the wave drag of the modified region and the interference drag were computed by equation (11) and added to the wave drag of the wing on the basic body from previous calculations. In both cases agreement with the Fourier series result is very good.

These computations were performed using only a slide rule and a planimeter, and yet the results agree well with the Fourier series method

[redacted]

where the Fourier series has converged satisfactorily. The method has the distinct advantage of being a flexible one, permitting the computer to work with greater care in critical regions and to achieve accuracy as good as the initial $S'(x_o, \beta \cos \theta)$ curves will permit.

CONCLUDING REMARKS

As might be expected from previous experience, the theory gives wave-drag results that are considerably higher than experiment at a Mach number of 1 for most cases. However, as the Mach number increases, the agreement between theory and experiment becomes very good for wing A and for wing B on the basic body. For wing B on the modified body, the computed wave drag departs from the experimental as the Mach number increases although the agreement is good near a Mach number of 1.

Consideration of the two computational methods used to evaluate the integrals indicates that the Fourier series technique has the advantage of speed and standardization when punched-card or other mechanized computing systems are available. When the gradient along the body axis of cross-sectional area of the configuration is smooth enough for a reasonable number of harmonics to provide a good fit to the curve, the Fourier series method gives satisfactory results. Care should be taken to check the goodness of fit, or the convergence of the series. The method based on Legendre's formula is not so fast and requires more attention to detail on the part of the computer, but it is very flexible and is certainly to be preferred in the absence of mechanized computing devices. Either the method based on Legendre's formula or the Fourier analysis can give a fairly rapid estimate of the effect of a component to be added to a basic configuration.

In general, the methods discussed in this report for evaluating the wave drag of a wing-body combination agree well among themselves and show good agreement with the experimental values when the configuration is sufficiently slender and when the derivative along the body axis of the area distribution is smooth.

Ames Aeronautical Laboratory
National Advisory Committee for Aeronautics
Moffett Field, Calif., Jan. 6, 1955

[redacted]

APPENDIX

DESCRIPTION OF COMPONENTS FOR WHICH COMPUTATIONS WERE PERFORMED

A. Basic body

for $0 < x < \frac{l}{2}$

$$r \cong r_o \left[1 - \left(1 - \frac{2x}{l} \right)^2 \right]^{3/4}$$

where

r_o = maximum radius = 1.875 inches

l = length of body = 43 inches

for $\frac{l}{2} < x < l$

$$r = r_o$$

B. Modified, or indented, body

for $0 < x < \frac{l}{2}$

same as basic body

for $\frac{l}{2} < x < l$

$r = r_o$ except in the region of the wing

where

$$S(x)_{body} = \pi r_o^2 - S(x)_{wing}$$

that is, the body was indented, still remaining circular in cross section, so that the cross-sectional area of the wing-body combination in planes perpendicular to the x axis was always equal to that of the basic body alone. In each case the wing was attached just back of the mid-point of the body.

[redacted]

C. Wing A

Wing tested by Whitcomb and described in reference 1 as "sweptback wing."

quarter-chord line swept back 45°

taper ratio = 0.6

aspect ratio = 4

NACA 65A006 sections in stream direction

span = 24 inches

wing area = 144 square inches

D. Wing B

Wing tested by Whitcomb and described in reference 1 as "unswept wing."

quarter-chord line unswept

taper ratio = 0

aspect ratio = 4

maximum thickness 4-percent chord

position of maximum thickness 40-percent chord

cross section in stream direction circular arcs

span = 24 inches

wing area 144 square inches

[redacted]

REFERENCES

1. Whitcomb, Richard T.: A Study of Zero-Lift Drag-Rise Characteristics of Wing-Body Combinations Near the Speed of Sound. NACA RM L52H08, 1952.

2. Hayes, Wallace D.: Linearized Supersonic Flow. North American Aviation, Inc. Rep. AL-222, June 18, 1947.

3. Heaslet, Max. A., Lomax, Harvard, and Spreiter, John R.: Linearized Compressible-Flow Theory for Sonic Flight Speeds. NACA Rep. 956, 1950.

4. von Kármán, Th.: The Problem of Resistance in Compressible Fluids (Fifth Volta Congress) Roma, Reale Accademia D'Italia, 1936.

5. Jones, Robert T.: Theory of Wing-Body Drag at Supersonic Speeds. NACA RM A53H18a, 1953.

6. Heaslet, Max. A., and Lomax, Harvard: Supersonic and Transonic Small Perturbation Theory. (Section D of General Theory of High Speed Aerodynamics. Vol. VI of High Speed Aerodynamics and Jet Propulsion, W. R. Sears, ed., Princton Univ. Press, 1954.)

7. Holdaway, George H.: Comparison of Theoretical and Experimental Zero-Lift Drag-Rise Characteristics of Wing-Body-Tail Combinations Near the Speed of Sound. NACA RM A53H17, 1953.

8. Sears, William R.: On Projectiles of Minimum Wave Drag. Quart. Appl. Math., vol. 4, no. 4, Jan. 1947, pp. 361-366.

9. Legendre, M. Robert: Aerodynamique - Limite Sonique de la Resistance d'ondes d'un aeronef. Comptes Rendus, Tome 236, No. 26, 29 Juni 1953, pp. 2479-2480.

10. Holdaway, George H.: An Experimental Investigation of Reduction in Transonic Drag Rise at Zero Lift by the Addition of Volume to the Fuselage of a Wing-Body-Tail Configuration and a Comparison With Theory. NACA RM A54F22, 1954.

11. Osborne, Robert S., and Mugler, John P.: Aerodynamic Characteristics of a 45° Sweptback Wing-Fuselage Combination and the Fuselage Alone Obtained in the Langley 8-Foot Transonic Tunnel. NACA RM L52E14, 1952.

[redacted]

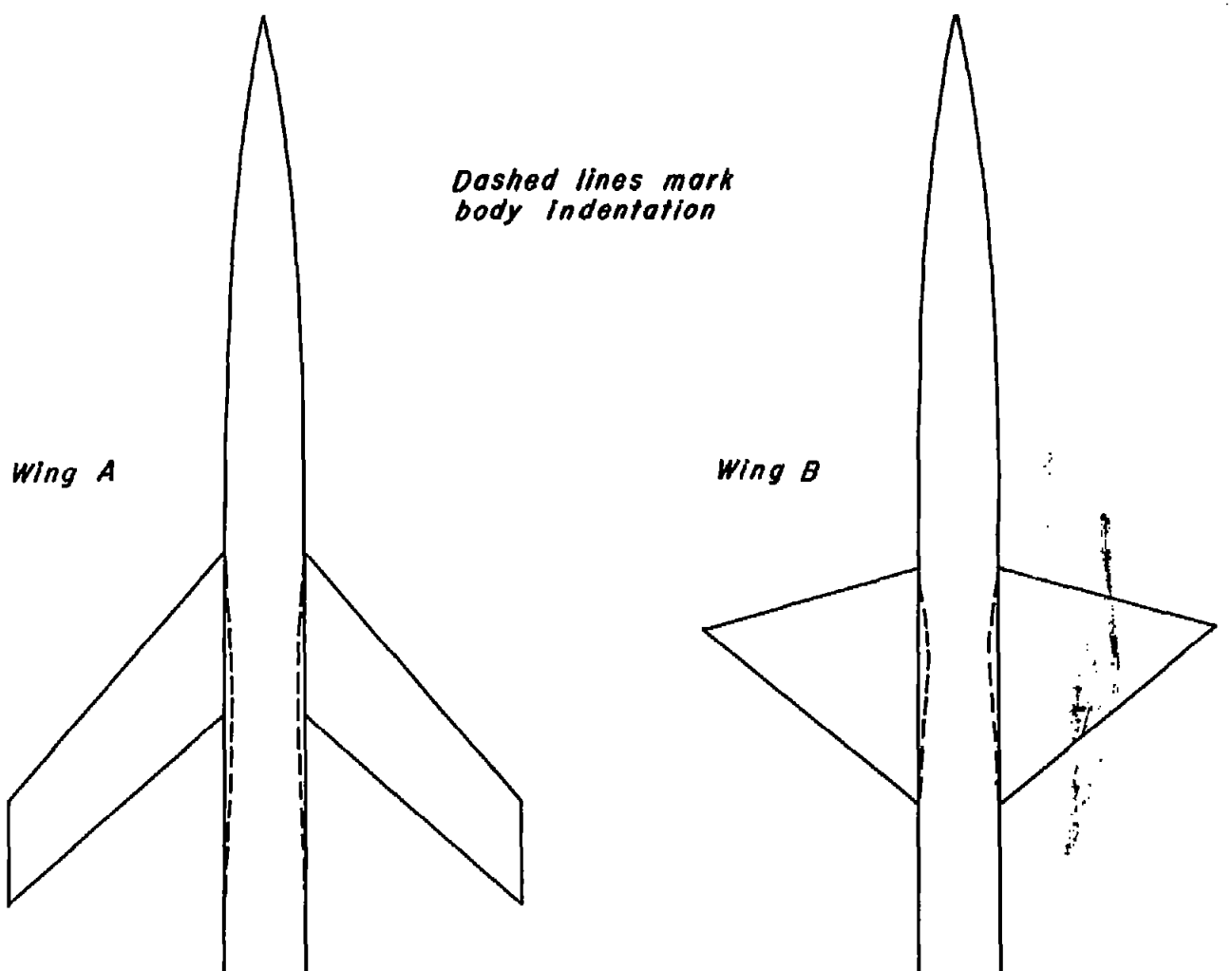

Figure 1.- Wing-body combinations considered in this report.

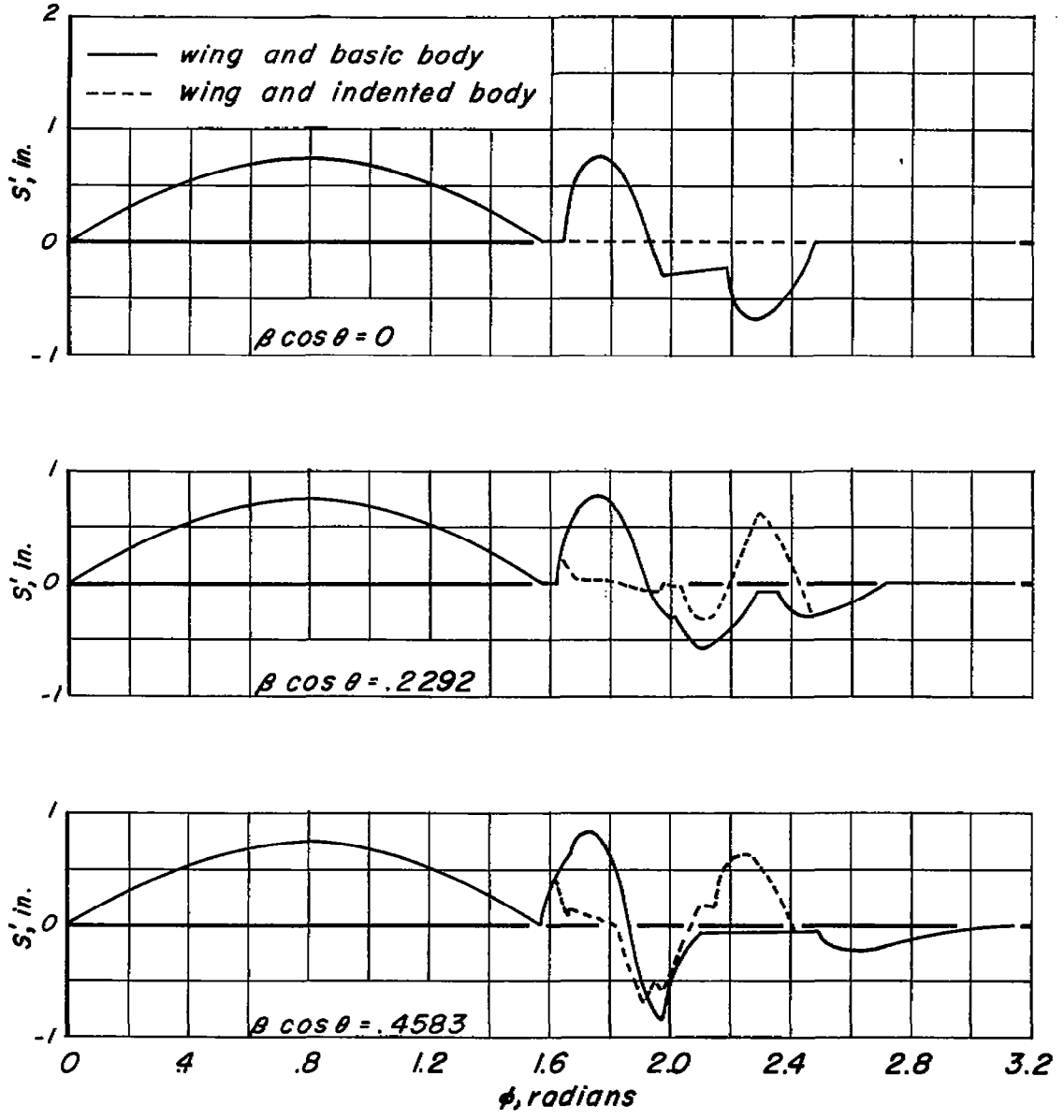

Figure 2.- Variation of $S'(x_o, \beta \cos \theta)$ with φ for wing A for three values of $\beta \cos \theta$.

[redacted]

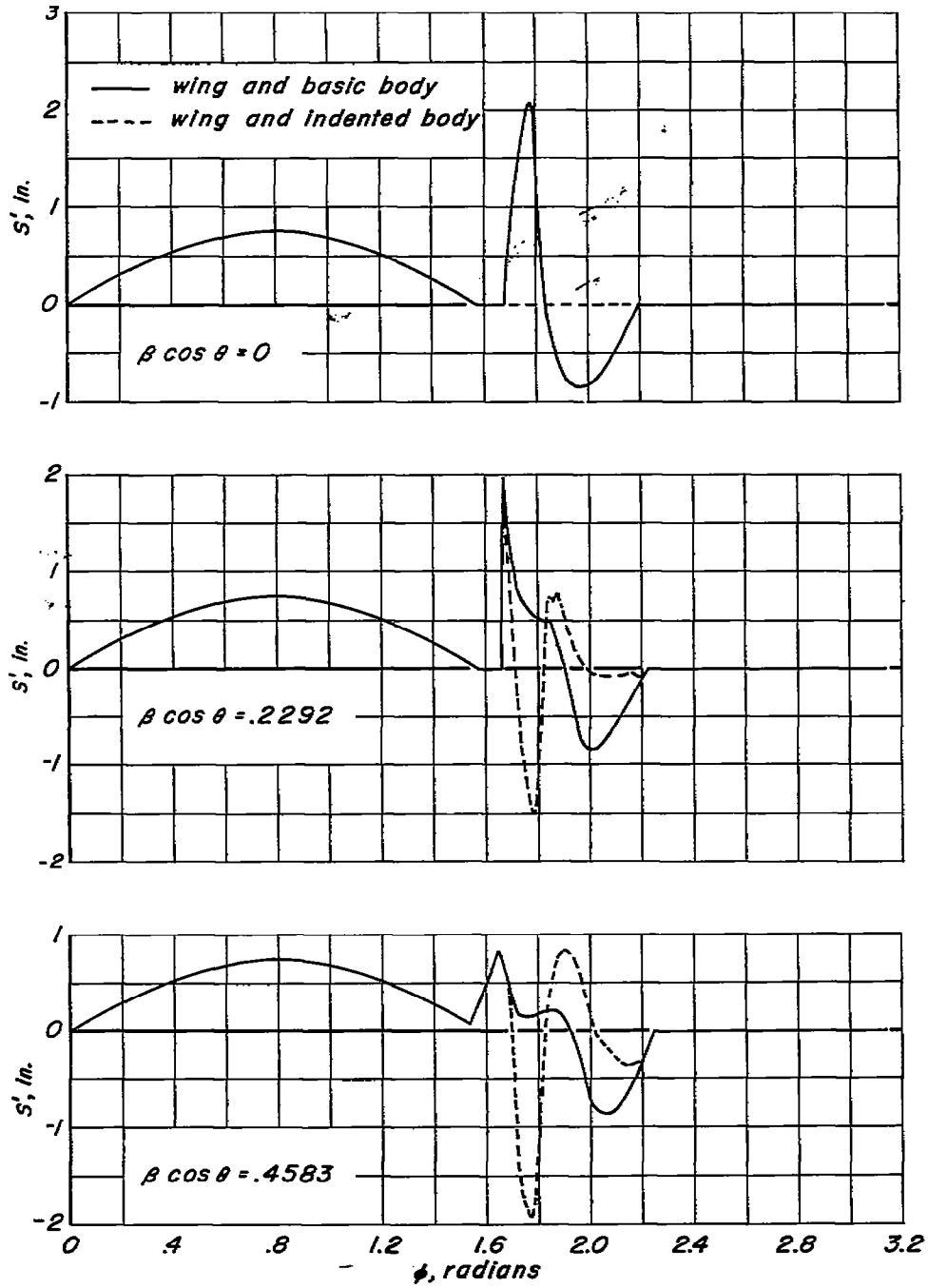

Figure 3.- Variation of $S'(x_o, \beta \cos \theta)$ with φ for wing B for three values of $\beta \cos \theta$.

[redacted]

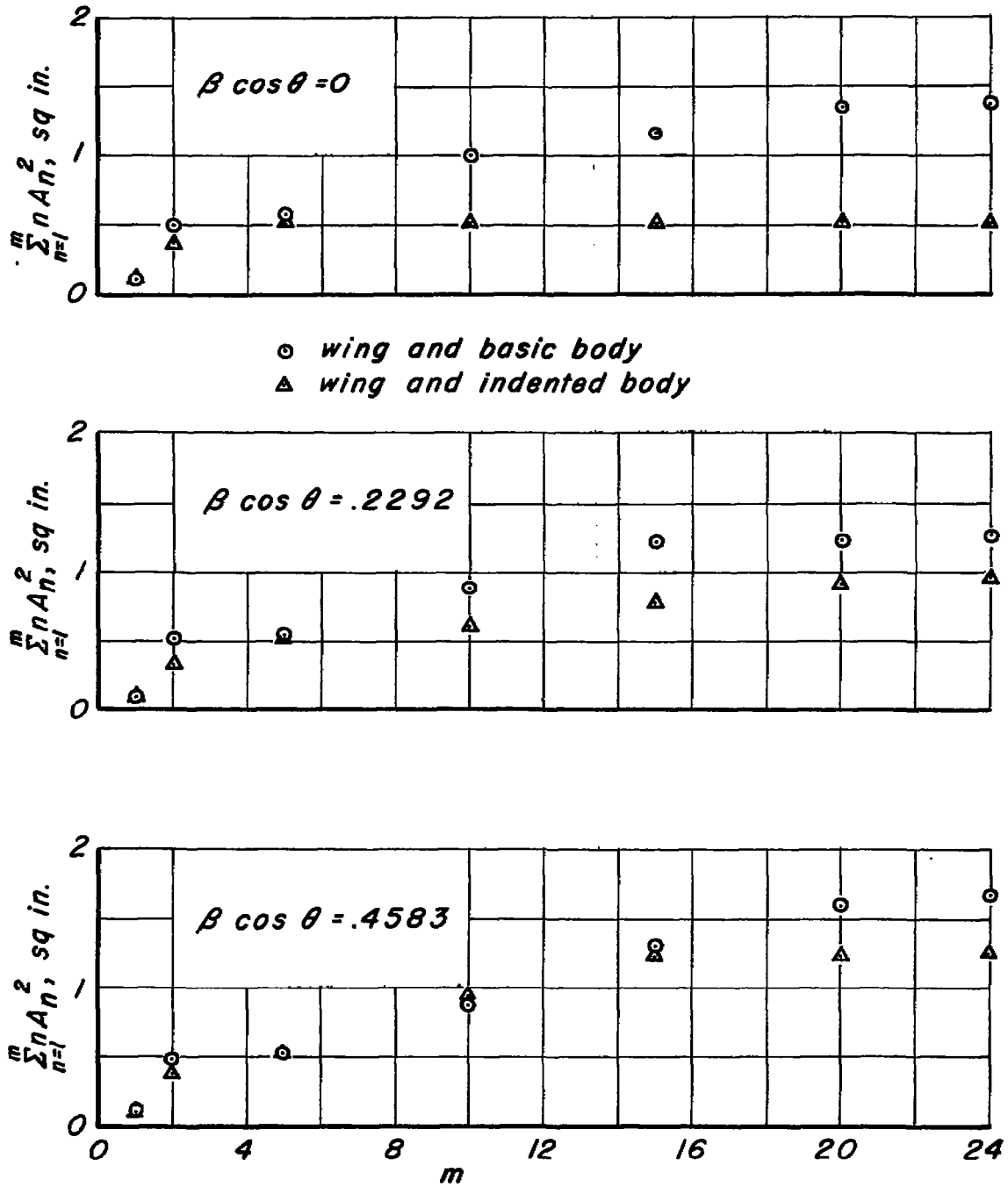

Figure 4.- Variation of $\sum_{n=1}^{m} nA_n^2$ with m for wing A for three values of $\beta \cos \theta$.

[redacted]

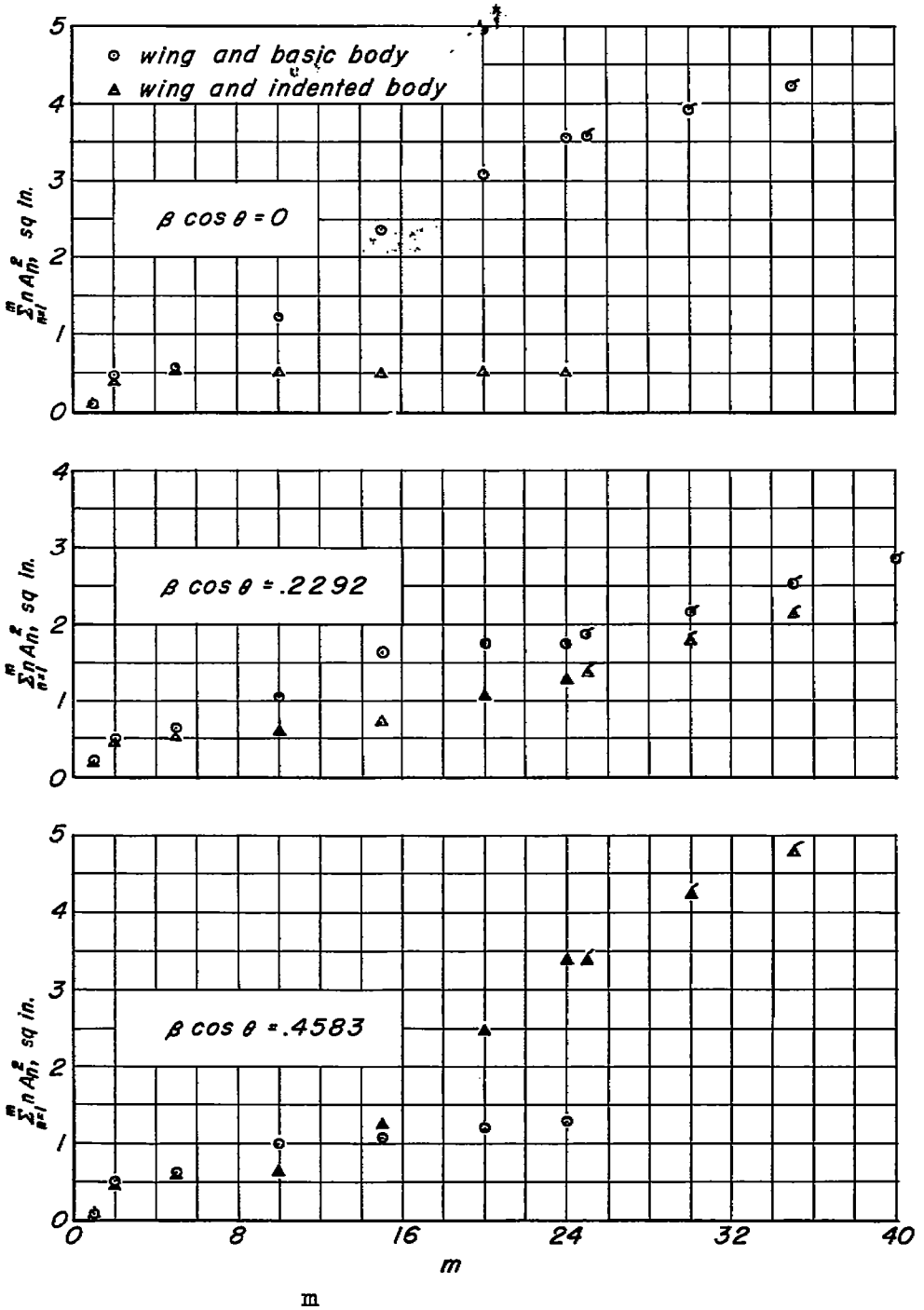

Figure 5.- Variation of $\sum_{n=1}^{m} nA_n^2$ with m for wing B for three values of $\beta \cos \theta$.

[redacted]

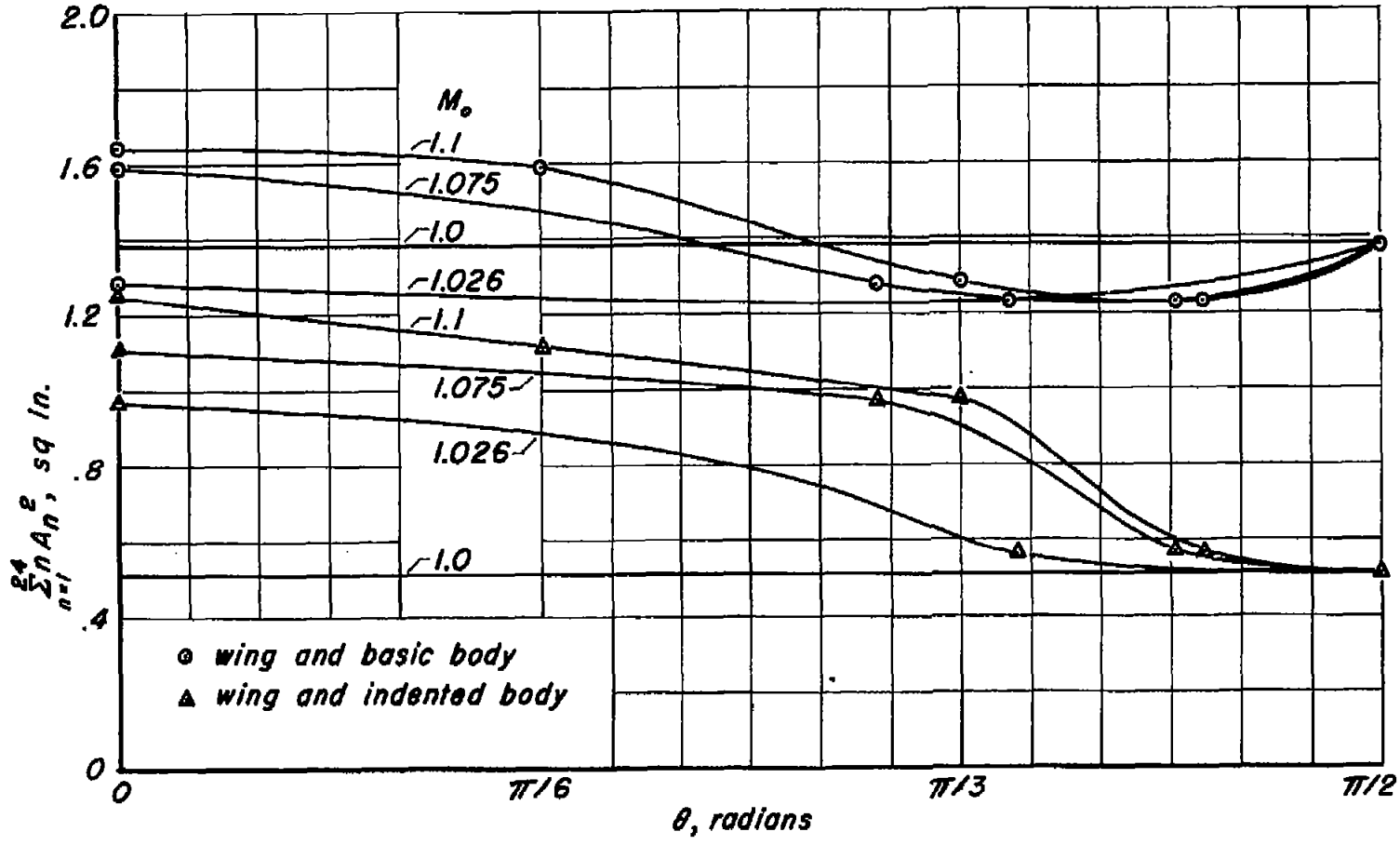

Figure 6.- Variation of $\sum_{n=1}^{24} nA_n^2$ with azimuth angle, θ, for wing A for four values of Mach number, M_o.

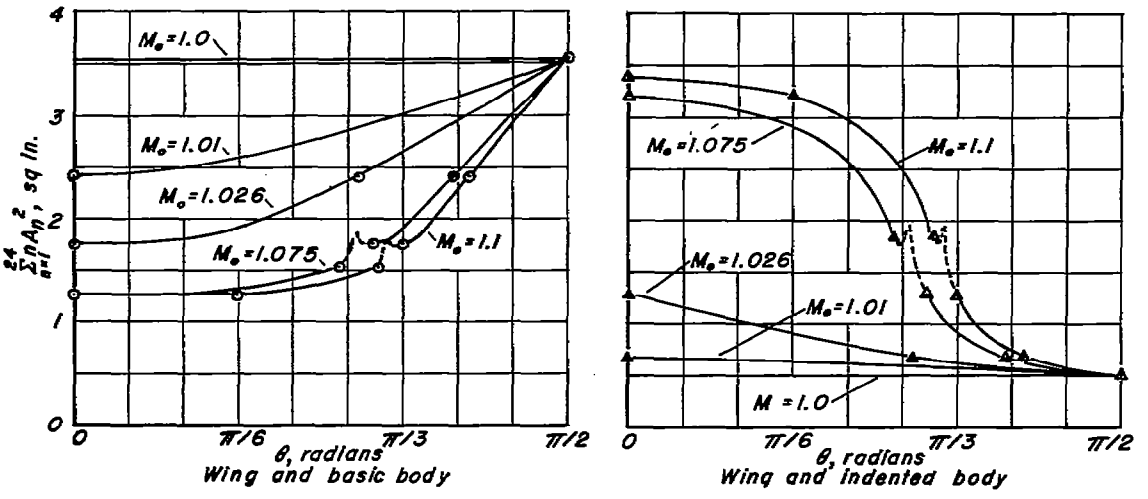

(a) 24 terms of Fourier series (m = 24)

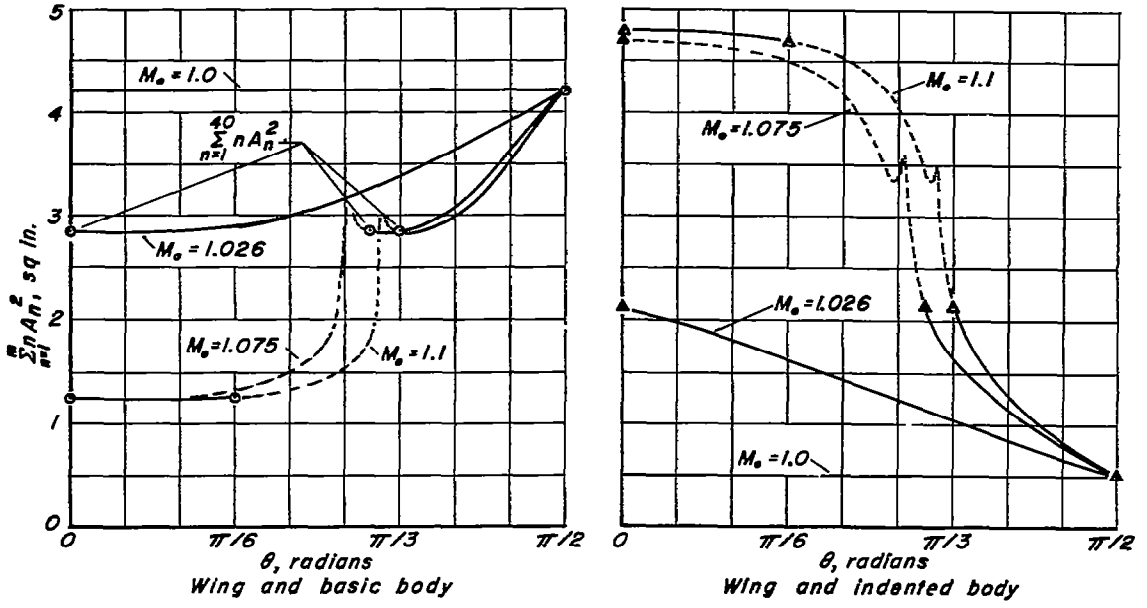

(b) 35 or more terms of Fourier series ($m \geq 35$)

Figure 7.- Variation of $\sum_{n=1}^{m} nA_n^2$ with azimuth angle, θ, for wing B for four values of Mach number M_o.

[redacted]

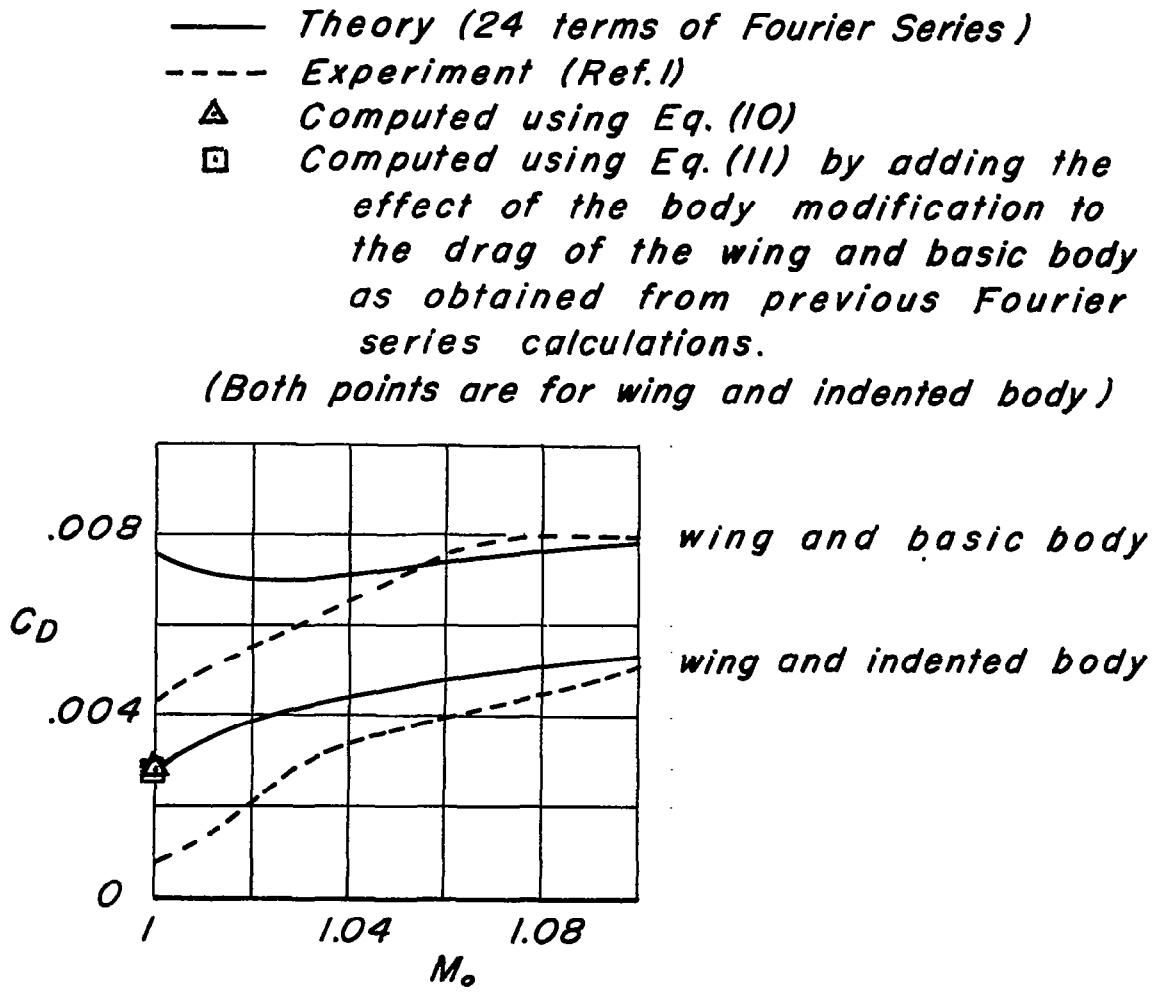

Figure 8.- Wave-drag coefficient vs. Mach number for wing A in combination with basic body and indented body.

[redacted]

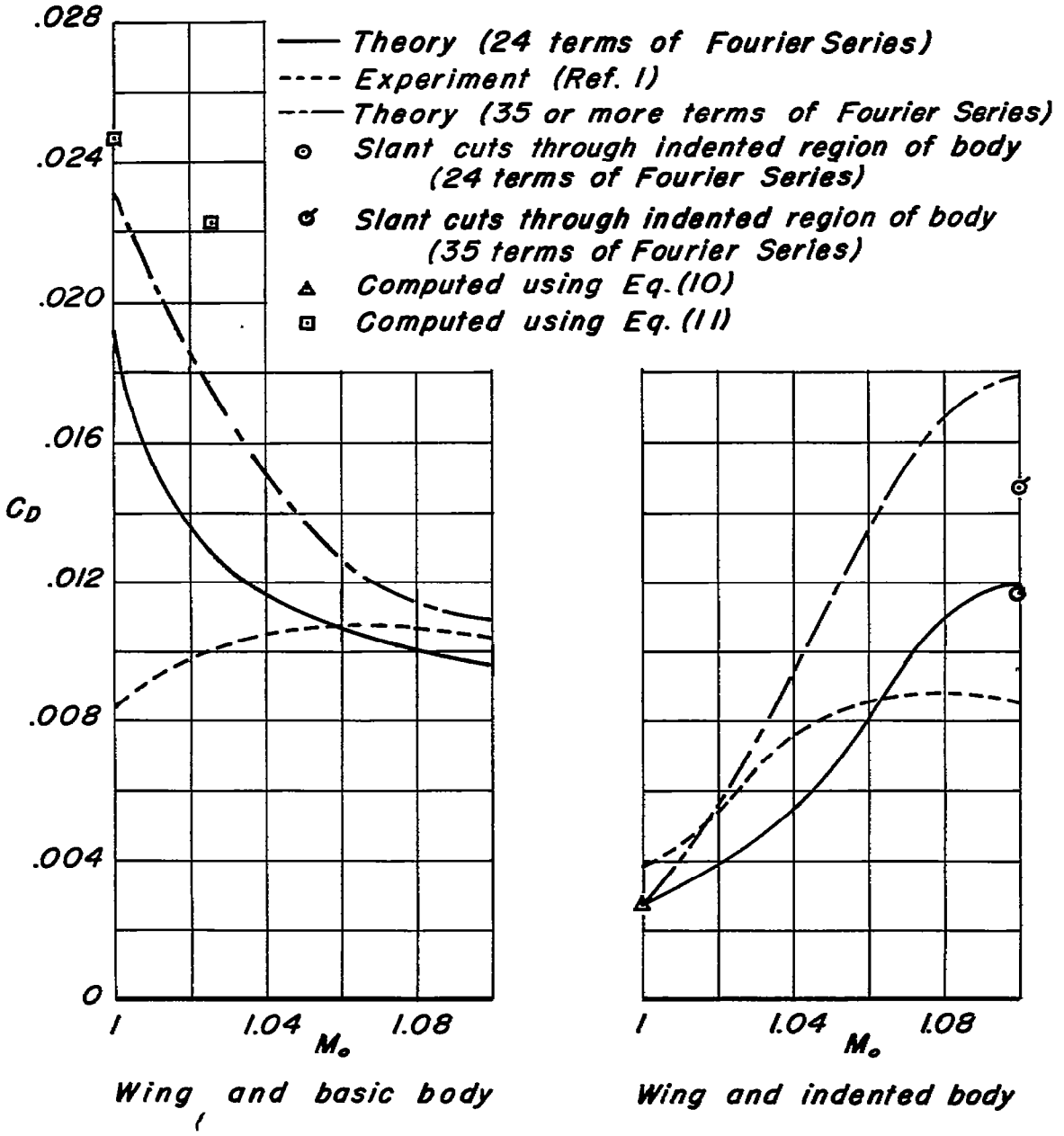

Figure 9.- Wave-drag coefficient vs. Mach number for wing B in combination with basic body and indented body.

[redacted]

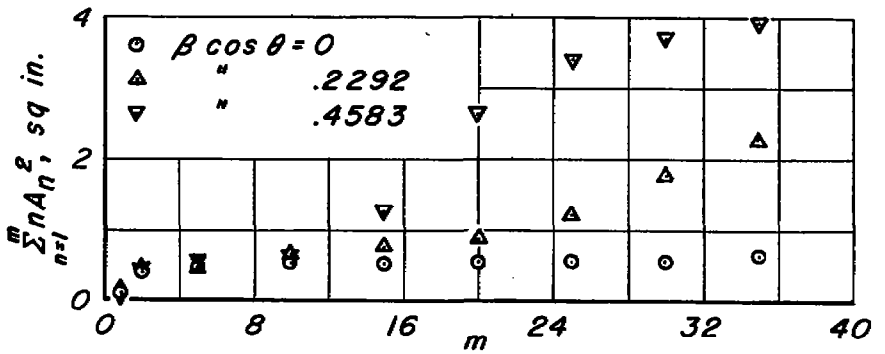

(a) $\sum_{n=1}^{m} nA_n^2$ vs m for three values of $\beta \cos \theta$. $M_o = 1.1$

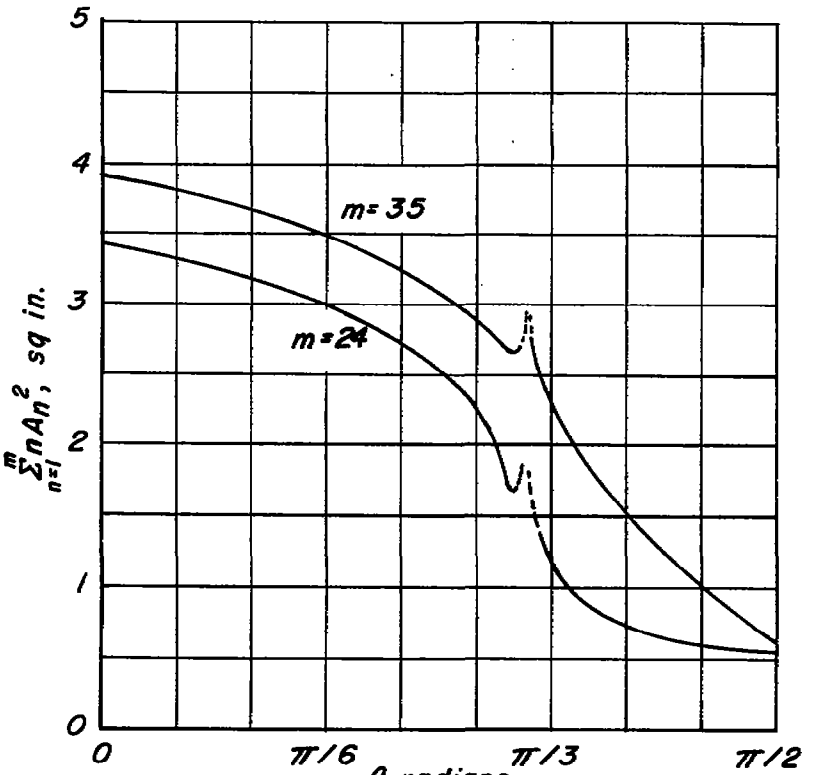

(b) $\sum_{n=1}^{m} nA_n^2$ vs θ for $M_o = 1.1$

Figure 10.- Intermediate steps in the evaluation of the wave drag of wing B on indented body at $M_o = 1.1$, using slant cuts through indented region of body.

[redacted]